


12-2011

## Field-controlled Electron Transfer and Reaction Kinetics of the Biological Catalytic System of Microperoxidase-11 and Hydrogen Peroxide

Yongki Chou  
*Cleveland State University*

Siu-Tung Yau  
*Cleveland State University, s.yau@csuohio.edu*

Follow this and additional works at: [https://engagedscholarship.csuohio.edu/enece\\_facpub](https://engagedscholarship.csuohio.edu/enece_facpub)

 Part of the [Biomedical Engineering and Bioengineering Commons](#), and the [Electrical and Computer Engineering Commons](#)

**How does access to this work benefit you? Let us know!**

---

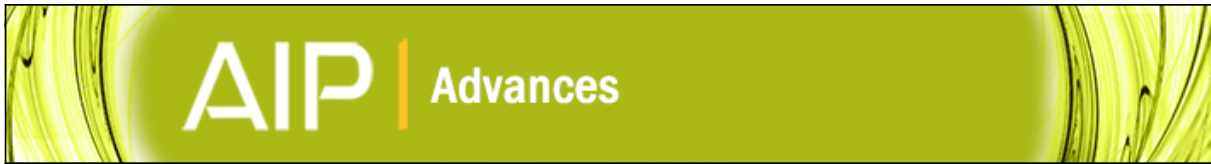
### Original Citation

Y. Choi and S. Yau. Field-controlled electron transfer and reaction kinetics of the biological catalytic system of microperoxidase-11 and hydrogen peroxide. *AIP Advances* 1(4), 2011. . DOI: <http://dx.doi.org/10.1063/1.3672093>.

### Repository Citation

Chou, Yongki and Yau, Siu-Tung, "Field-controlled Electron Transfer and Reaction Kinetics of the Biological Catalytic System of Microperoxidase-11 and Hydrogen Peroxide" (2011). *Electrical Engineering and Computer Science Faculty Publications*. 219.  
[https://engagedscholarship.csuohio.edu/enece\\_facpub/219](https://engagedscholarship.csuohio.edu/enece_facpub/219)

This Article is brought to you for free and open access by the Electrical and Computer Engineering Department at EngagedScholarship@CSU. It has been accepted for inclusion in Electrical Engineering and Computer Science Faculty Publications by an authorized administrator of EngagedScholarship@CSU. For more information, please contact [library.es@csuohio.edu](mailto:library.es@csuohio.edu).



## Field-controlled electron transfer and reaction kinetics of the biological catalytic system of microperoxidase-11 and hydrogen peroxide

Yongki Choi and Siu-Tung Yau


Citation: [AIP Advances](#) **1**, 042175 (2011); doi: 10.1063/1.3672093

View online: <http://dx.doi.org/10.1063/1.3672093>

View Table of Contents: <http://scitation.aip.org/content/aip/journal/adva/1/4?ver=pdfcov>

Published by the [AIP Publishing](#)

---



*Read Articles Now!*

**Special Topic: Physics in China**  
A focus of materials physics research

Engge Wang,, Xincheng Xie, Qikun Xue, Guest Editors

# Field-controlled electron transfer and reaction kinetics of the biological catalytic system of microperoxidase-11 and hydrogen peroxide

Yongki Choi<sup>1,2</sup> and Siu-Tung Yau<sup>1,a</sup>

<sup>1</sup>*Department of Electrical and Computer Engineering and The Applied Bioengineering Program, Cleveland State University, Cleveland, Ohio 44115, USA*

<sup>2</sup>*Department of Physics and Astronomy, University of California Irvine, Irvine, California 92697-4575, USA*

(Received 11 June 2011; accepted 4 December 2011; published online 12 December 2011)

Controlled reaction kinetics of the bio-catalytic system of microperoxidase-11 and hydrogen peroxide has been achieved using an electrostatic technique. The technique allowed independent control of 1) the thermodynamics of the system using electrochemical setup and 2) the quantum mechanical tunneling at the interface between microperoxidase-11 and the working electrode by applying a gating voltage to the electrode. The cathodic currents of electrodes immobilized with microperoxidase-11 showed a dependence on the gating voltage in the presence of hydrogen peroxide, indicating a controllable reduction reaction. The measured kinetic parameters of the bio-catalytic reduction showed nonlinear dependences on the gating voltage as the result of modified interfacial electron tunnel due to the field induced at the microperoxidase-11-electrode interface. Our results indicate that the kinetics of the reduction of hydrogen peroxide can be controlled by a gating voltage and illustrate the operation of a field-effect bio-catalytic transistor, whose current-generating mechanism is the conversion of hydrogen peroxide to water with the current being controlled by the gating voltage. *Copyright 2011 Author(s). This article is distributed under a Creative Commons Attribution 3.0 Unported License.* [doi:[10.1063/1.3672093](https://doi.org/10.1063/1.3672093)]

## I. INTRODUCTION

Electron transfer is a fundamental process, which is responsible for important biological phenomena such as photosynthesis, respiration and metabolism. The pertinent electron transfer process in biological and chemical systems is long-range electron transfer (LRET).<sup>1–3</sup> LRET occurs over a distance on the order of 10 Å in biological systems,<sup>4</sup> where electrons tunnel between electroactive donors and acceptors through polypeptide networks. According to the Marcus electron transfer theory,<sup>1,5</sup> the rate constant  $k_{et}$  of tunneling between a pair of weakly coupled donor and acceptor depends critically on two parameters,<sup>5</sup> i.e.

$$k_{et} \propto \exp(-\beta d) \quad (1)$$

where  $d$  is the distance in the insulating barrier between the donor and the acceptor and  $\beta$  is the attenuation coefficient, which is proportional to the square root of the tunnel barrier height ( $\beta \propto (\Phi_0)^{1/2}$ ).<sup>5</sup> The LRET formalism is used in the pathway model of electron transfer in the biological systems to describe the strength of both through-bond<sup>6</sup> and through-space<sup>4</sup> coupling routes from donors to acceptors.<sup>7</sup>

Effectively controlled electron transfer is one of the primary regulation mechanisms in biology and biomolecular machines,<sup>8,9</sup> while efficiently controlled reaction kinetics of biological catalysis

<sup>a</sup>Author to whom correspondence should be addressed. Electronic mail: [s.yau@csuohio.edu](mailto:s.yau@csuohio.edu), Fax: (216) 678-5405



is an essential requirement for viable renewable and green energy processes.<sup>10</sup> Two approaches have been developed to modify proteins in order to control LRET in proteins. In the first approach, the rate of electron transfer is altered by choosing the medium intervening between the donor and the acceptor.<sup>11,12</sup> The intervening molecule covalently links the donor and the acceptor. In the second approach, a redox-active inorganic complex is covalently attached to the surface of a redox protein to facilitate intraprotein electron transfer between centers covalently linked to well-defined sites within a protein.<sup>13–16</sup>

Presently, extrinsic control of electron transfer and reaction kinetics in biological systems is performed mainly optically.<sup>17</sup> Optical techniques are incompatible with the manipulation of the properties of discrete nanoscale biological systems. Recently, it was proposed that, by controlling the rate of electron transfer in metabolic systems using certain chemical reactions, metabolism can be regulated to avoid detrimental oxidative stress effects.<sup>18</sup> It was predicted that the activation energy that determines electron transfer efficiency across a biological membrane can be controlled using electrostatic means.<sup>19</sup> Until now, the only demonstrated electrostatic control of electron transfer in proteins was the change in the interfacial current as the result of the reorientation of cytochrome c on the working electrode caused by the electrochemical cell potential.<sup>20–22</sup>

Recently, we have demonstrated that the anodic signal currents of glucose and ethanol enzymatic biosensors can be enhanced by applying a voltage to the enzyme immobilized on the sensors' electrodes.<sup>23</sup> The effect was used to obtain ultrasensitive detection of substances on the pico-molar level. Here, we show that the electron transfer associated with the electro-reduction of hydrogen peroxide ( $\text{H}_2\text{O}_2$ ) catalyzed by microperoxidase-11 (MP-11), a redox biomolecule, that is immobilized on an electrode can be manipulated by applying an electric field to the biomolecule via an external gating voltage. MP-11 and  $\text{H}_2\text{O}_2$  is an important bio-catalytic system. MP-11 is a heme-containing oligopeptide that consists of the active site microenvironment of cytochrome c, an electron transfer protein for many redox enzymes.  $\text{H}_2\text{O}_2$ , a strong oxidizing agent, is produced in organisms as a byproduct of oxygen metabolism. Biomolecule such as MP-11 catalyzes the reduction of hydrogen peroxide to water<sup>24</sup> and therefore reduces oxidative stress. The most important result of this work is the nonlinear dependences of the kinetic parameters of the catalysis on the gating voltage, implying an efficiently controlled substance conversion process.

## II. EXPERIMENTAL METHODS

The experimental setup is described in Figure 1(a). The principle of the experimental setup is described below and in ref. 23. The experimental setup consists of a conventional three-electrode electrochemical cell with a cell potential  $V_{\text{cell}}$  connected between the working electrode and the reference electrode. The cell is modified with additional gating electrodes for applying an external gating voltage  $V_G$  between the gating electrodes and the working electrode, upon which redox molecules are immobilized. The molecules were immobilized within an area of  $1\text{ mm} \times 1\text{ mm}$  on the bare edge-plane of a highly oriented pyrolytic graphite (HOPG) electrode.<sup>25</sup> A piece of 0.5 mm-diameter copper wire coated with a thin layer of insulator (enamel) was used as the gating electrode. The wire was bent to form a U-shaped structure, which was attached on the working electrode next to the immobilized enzyme molecules. The cell was driven by a commercial electrochemical controller (CHI 660C). A commercial Ag/AgCl (3 M KCl) electrode was used as the reference electrode, and a platinum wire was used as the counter electrode. A potential scan rate of 50 mV/s was used in recording cyclic voltammograms (CV). Microperoxidase-11 (MP-11), Fe(III)-protoporphyrin IX (FePP) and hydrogen peroxide were purchased from Sigma and used as received. MP-11 solution was made by dissolving 1 mg of MP-11 in 1 mL of 100 mM phosphate buffer (42mM  $\text{NaH}_2\text{PO}_4 \cdot \text{H}_2\text{O}$ , 58mM  $\text{Na}_2\text{HPO}_4 \cdot 7\text{H}_2\text{O}$ , pH 7.0). To form a molecule-immobilized electrode, a 0.1 ml drop of the MP-11 solution or a 0.1 ml drop of 100  $\mu\text{M}$  FePP solution in 10 mM sodium borate buffer ( $\text{Na}_2\text{B}_4\text{O}_7 \cdot 10\text{H}_2\text{O}$ , pH 10) was deposited on the edge plane of HOPG surface, which was then incubated at room temperature for 4 hours. It is known that FePP is a hydrophobic molecule<sup>26</sup> and MP-11 contains surface hydrophobic residues.<sup>27</sup> Since the edge plan of the HOPG electrode was produced by scratching the basal plan, which is hydrophobic, the contact of the electrode surface with the molecules has most likely resulted in molecular adsorption due to hydrophobic interaction

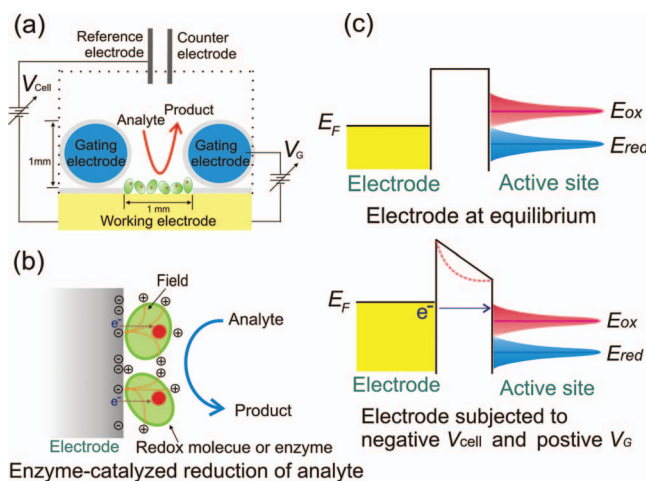


FIG. 1. The principle of the field-modulation technique. (a) Experimental setup (cross-sectional view). Each elliptical structure represents a redox molecule, whose active center is indicated by the smaller circle within a molecule. The gating electrodes are represented by the circular structures, which consist of a copper wire (the blue circles) and a thin layer of insulator (the shaded shells). (b) The ion-induced electric field at the solution-electrode interface. The brown arrow indicates the direction of electron transfer and the orange arrow indicates the direction of the electric field (c) Energy profile of the molecule-electrode interface.  $E_{red}$  and  $E_{ox}$  are respectively the most probable energies for the occupied and unoccupied quantum states of the active site. The Gaussian-shaped regions are the distributions associated with these energies.  $E_F$  is the Fermi energy of the electrode.

between the molecules and the basal plan residues. CVs of MP-11 immobilized electrode shows that the MP-11 molecule forms a monolayer on the electrode.<sup>28</sup> All measurements were made with deaerated phosphate buffer and sodium borate buffer at room temperature.

### III. RESULTS AND DISCUSSION

#### A. Interfacial electron transfer of Fe(III)-protoporphyrin IX

A study on the interfacial electron transfer characteristics of Fe(III)-protoporphyrin IX (FePP), an organic redox molecule, was carried out using the experimental setup in order to demonstrate the feasibility of using the experimental approach to control bio-catalytic reactions. Iron-porphyrin complexes such as FePP form the prosthetic group (the heme ( $\text{Fe}^{3+}/\text{Fe}^{2+}$ )) of a number of electroactive proteins such as hemoglobin and cytochrome c that are often encountered in biological electron transfer processes.<sup>29</sup> These heme-containing proteins exhibit a wide range of biological functions, including simple electron transfer reactions, oxygen transport and storage, oxygen reduction to the level of hydrogen peroxide or water, and the reduction of peroxides.<sup>24</sup> The redox reaction of FePP immobilized on an electrode has been intensively studied.<sup>30</sup> Cyclic voltammograms (CVs) of a HOPG electrode immobilized with FePP were obtained under different conditions as shown in Figure 2(a). The black CV, obtained with  $V_G = 0$  V, shows a pair of redox peaks with a formal potential of  $E^0 = -0.5$  V (vs. Ag/AgCl), indicating the molecule's electron transfer (redox) reaction, in which  $\text{Fe}^{3+}$  is reversibly reduced to  $\text{Fe}^{2+}$  as previously reported.<sup>30</sup> When  $V_G$  is increased to 0.2 V, the corresponding red CV shows a slight downward shift with increased redox peak currents. The blue CV corresponds to a more positive  $V_G$  of 0.8 V. It shows further increases in the redox peak currents. Figure 2(b) shows detailed increases in the anodic peak and cathodic peak currents described in Figure 2(a). The dashed baselines are used to indicate the changes in the peak currents. The inset of Figure 2(a) shows the dependence of the peak currents on  $V_G$ . In the inset, the blue double-headed line is used to indicate the reversibility of this dependence with  $V_G$ . Therefore, the inset shows the manipulation of the interfacial electron transfer. Note that control experiments performed using bare electrodes with and without  $V_G$  showed no characteristics similar to those obtained in the presence of redox molecules as displayed in Figures 2 and 3.

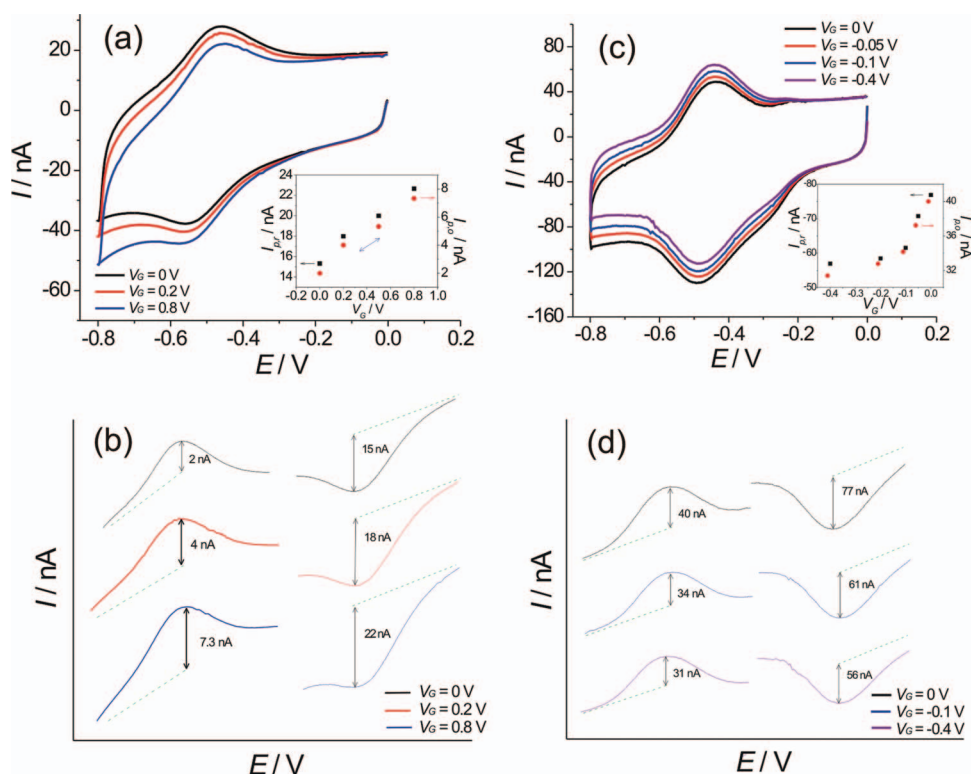


FIG. 2. The effect of  $V_G$  on the redox properties of FePP immobilized on an electrode. (a) The CVs were obtained in 10 mM sodium borate buffer ( $\text{Na}_2\text{B}_4\text{O}_7 \cdot 10\text{H}_2\text{O}$ , pH 10) with different values of  $V_G$ . The inset shows the manipulation of the redox peak currents by varying  $V_G$ .  $I_{p,o}$  and  $I_{p,r}$  are the peak currents of the oxidation peak and the reduction peak, respectively. (b) Detailed increases in the anodic peak and cathodic peak currents in (a). (c) The CVs were obtained using a different FePP electrode under the same conditions as in (a) with the polarity of  $V_G$  reversed. The inset shows the dependences of the peak currents on  $V_G$ . The peak currents of the redox peaks of FePP decrease as the magnitude of the reversed  $V_G$  is increased, indicating an increased effective height of the tunnel barrier. (d) Detailed decreases in the anodic peak and cathodic peak currents in (c). In the figures, the green dashed lines are used to indicate the baselines for estimating the peak heights, which are indicated by the solid lines with double arrows.

For redox molecules immobilized on an electrode, quantum mechanical tunneling gives rise to interfacial electron transfer between the molecules and the electrode. Since the active site of a redox molecule is usually surrounded by a non-electroactive molecular network, interfacial electron transfer is facilitated by electron tunneling and the molecular network forms the tunneling barrier. It is known that the electronic energy profile of an insulating material can be modified by an electric field,<sup>31</sup> and this effect has recently been used to construct a field-effect transistor using a non-electroactive protein as the active material.<sup>32</sup> The observed increased redox peak currents due to  $V_G$  is consistent with the scenario that the electronic energy profile of the tunnel barrier (the non-electroactive part of FePP surrounding the  $\text{Fe}^{3+}/\text{Fe}^{2+}$  site) at the molecule-electrode interface is modified by an electric field so that the tunneling rate is enhanced. In our experimental setup, for positive values of  $V_G$ , negative charges are induced on the surface of the HOPG electrode and positive ions are induced at the interface between the solution and the molecules, establishing electric fields within the molecule as shown in Figure 1(b). This field reduces the effective height of the tunnel barrier and therefore enhances the rate of tunneling.<sup>33</sup>

Figure 1(c) shows a conceptual electronic energy-band diagram of the molecule-electrode interface. Consider the reduction process of the molecule. Thermodynamic consideration shows that, at equilibrium, no electron transfer occurs between the electrode and the active site, since the energy of the lowest unoccupied quantum state of the active site,  $E_{ox}$ , is above the Fermi energy  $E_F$  of the electrode. When  $V_{\text{cell}}$  is applied such that the potential of the working electrode is below that of the reference electrode, reduction of the molecule occurs as electrons are energetically allowed



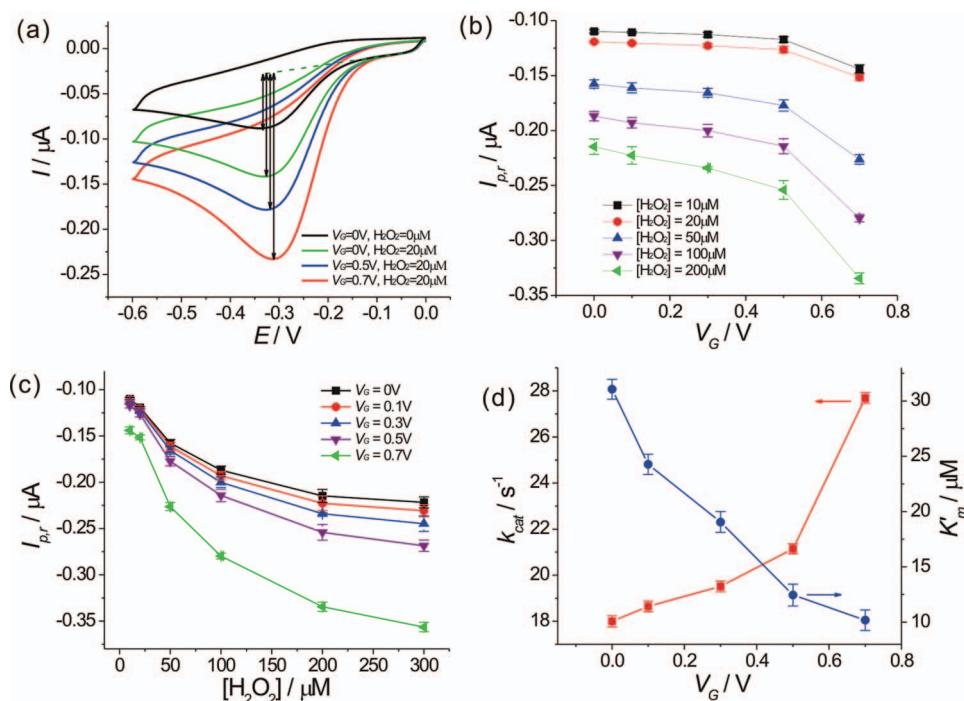


FIG. 3. The effect of  $V_G$  on the reduction of  $\text{H}_2\text{O}_2$  catalyzed by MP-11. (a) CVs of immobilized MP-11 obtained in 100 mM phosphate buffer (42mM  $\text{NaH}_2\text{PO}_4 \cdot \text{H}_2\text{O}$ , 58mM  $\text{Na}_2\text{HPO}_4 \cdot 7\text{H}_2\text{O}$ , pH 7.0) under different conditions. The green dashed line is used to indicate the baseline for estimating the reduction peak heights, which are indicated by the solid lines with double arrows. The CVs were obtained consecutively with the same electrode. (b) The dependence of  $I_{p,r}$  on  $V_G$  for different  $\text{H}_2\text{O}_2$  concentrations. (c) The  $\text{H}_2\text{O}_2$  calibration curves of the MP-11-immobilized electrode for different value of  $V_G$ . (d) The dependences of  $K'_m$  and  $k_{\text{cat}}$  on  $V_G$ .

to be transferred from the electrode to  $E_{\text{ox}}$ . The electrode-active site system can be considered as a acceptor-donor pair and  $k_{\text{et}} \propto \exp(-\beta d)$ . In general,  $d$  can be large so that electron transfer is diminished. The size of the non-electroactive part for FePP is about 5 Å and that for MP-11 is about 12 Å, which are fixed. However,  $\beta$ , which is determined by the effective height of the tunnel barrier, can be reduced using the  $V_G$ -induced field as described in Figure 1(b). The field distorts the top of the tunnel barrier (see the red dashed curve in Figure 1(c)), reducing the effective height of the barrier and, therefore, resulting in a smaller value of  $\beta$  and a larger value of  $k_{\text{et}}$ . Thus, the observed increases in the redox peak currents of the immobilized FePP and the reduction current of  $\text{H}_2\text{O}_2$  catalyzed by MP-11 (see below) are likely to be the result of the field-induced modification of the energy barrier for tunneling. To provide additional evidence for this scenario, we performed the above experiment with the polarity of  $V_G$  reversed. As shown in Figure 2(c), the redox peak currents of FePP decrease as the magnitude of the reversed voltage is increased, indicating an increased effective height of the tunnel barrier. Figure 2(d) shows detailed decreases in the anodic peak and cathodic peak currents described in Figure 2(c).<sup>29</sup> The inset of Figure 2(c) shows the dependence of the peak currents on  $V_G$ . Figure 1(c) shows that the experimental system as described in Figure 1(a) provides independent controls of the two aspects of the electron transfer process of the system, namely, the thermodynamic properties of the electrode reaction and the quantum mechanical tunneling at the molecule-electrode interface.

A closer examination of the CVs of Figure 2(a) reveals the nature of the electrode reaction. Figure 2(a) shows that as  $V_G$  is increased, the redox currents increase while the peak-peak separation appears to be unchanged. This observation suggests that the electrode redox reaction is close to or in the irreversible regime, where the current depends on the product of  $k$  and  $\exp(k)$  while the half-wave electrode potential depends on  $\ln(k)$ ,  $k$  being the reaction rate constant.<sup>34</sup> When  $V_G$  is increased,  $k_{\text{et}}$  is also increased as explained above. Since, in the microscopic theory of charge transfer,<sup>34</sup>  $k$

is proportional to  $k_{et}$ , the increased  $k_{et}$  makes  $k$  and therefore the current increase as shown in Figure 2(a). However, the  $\ln(k)$ -dependence makes the peak-peak separation less sensitive to the increase in  $k_{et}$ .

## B. Field-controlled catalytic electron transfer at the MP-11-electrode interface

We have performed cyclic voltammetry of MP-11-immobilized electrodes to characterize the redox properties of MP-11.<sup>29</sup> The electro-reduction of  $\text{H}_2\text{O}_2$  catalyzed by MP-11 and affected by  $V_G$  is described in Figure 3. Figure 3(a) shows the bio-catalytic activities of a MP-11-immobilized electrode for  $\text{H}_2\text{O}_2$  in the absence and presence  $V_G$ . The black CV shows the electrode's behavior in the absence of  $\text{H}_2\text{O}_2$  and  $V_G$ . A pair of redox peaks is present in the CV with a formal potential of -0.25 V. Note that the weak anodic peak at -0.2 V indicate a quasi-reversible electrode redox reaction, which is close to the irreversible limit with slow re-oxidation of the heme iron. The bio-catalytic nature of the electrode to  $\text{H}_2\text{O}_2$  is reflected in the green CV, which was obtained in 20  $\mu\text{M}$  of  $\text{H}_2\text{O}_2$ . The green CV, compared to the black CV, shows a large increase in the cathodic current, which is indicative of the reduction of  $\text{H}_2\text{O}_2$  to water and has been reported previously.<sup>35,36</sup> When  $V_G$  was turned on, the reduction current further increased as reflected in the blue and red CVs. This effect is consistent with the situation described in Figure 1(c) and the discussion on the enhanced electron transfer due to the reduced effective tunnel barrier height given above. Note that MP-11 performs the reduction by turning its ionization state from  $\text{Fe}^{3+}$  to  $\text{Fe}^{4+}$ . The  $\text{Fe}^{4+}$  state then returns to  $\text{Fe}^{3+}$  by receiving two electrons from the electrode through a two-step process, which involves the formation of a complex.<sup>37</sup> This way, the MP-11 electrode is able to reduce  $\text{H}_2\text{O}_2$  in the subsequent scans.

The dependence of the reduction peak current  $I_{p,r}$  on  $V_G$  at different concentrations of  $\text{H}_2\text{O}_2$  was measured and is displayed in Figure 3(b). It is obvious that, at a given  $\text{H}_2\text{O}_2$  concentration, increasing  $V_G$  causes  $I_{p,r}$  to increase. Thus, Figure 3(b) shows that the catalyzed reduction of  $\text{H}_2\text{O}_2$  by MP-11 can be controlled using  $V_G$ . Figure 3(c) shows the measured dependence of  $I_{p,r}$  on  $\text{H}_2\text{O}_2$  concentration for different values of  $V_G$ . The black curve is the electrode's intrinsic calibration curve for  $\text{H}_2\text{O}_2$ . It shows a linear dependence for low concentrations (10 ~ 50  $\mu\text{M}$ ) and a transition toward saturation at higher concentrations. This behavior indicates the Michaelis-Menten kinetics of the reduction process. All of the other curves, the  $V_G$ -dependent calibration curves, follow the same behavior with progressive downward shifts.

## C. Field-controlled reaction kinetics of the electro-reduction of hydrogen peroxide catalyzed by MP-11

To gain insight into the observed effect of  $V_G$  on the reduction reaction of  $\text{H}_2\text{O}_2$ , an investigation on the kinetic properties of the reaction has been made. The kinetics of the bio-catalytic conversion occurring at the electrode can be characterized using two parameters, namely,  $k_{cat}$  and  $K'_m$ , where  $k_{cat}$ , the turnover rate constant, is the maximum number of  $\text{H}_2\text{O}_2$  molecules that can be converted to water per second per active site and  $K'_m$  is the apparent Michaelis constant<sup>38</sup> obtained with MP-11 immobilized on the electrode and subjected to the field.  $K'_m$  is the  $\text{H}_2\text{O}_2$  concentration required for the velocity of the bio-catalytic conversion to reach half of its maximum velocity.<sup>39</sup> A low  $K'_m$  indicates high bio-catalytic efficiency of MP-11.<sup>39</sup> The Lineweaver-Burk (LB) equation relates  $I_{p,r}$ ,  $k_{cat}$  and  $K'_m$  as,<sup>40</sup>

$$1/I_{p,r} = \{K'_m/(nFAk_{cat}\Gamma[\text{H}_2\text{O}_2]) + 1/(nFAk_{cat}\Gamma)\} \quad (2)$$

where,  $n$  is number of electrons exchanged,  $F$  is the faraday constant,  $A$  is the electrode surface area, and  $\Gamma$  is the electrode's surface coverage by the MP-11. The numerical values of these constants used in this work are contained in Supplementary materials.<sup>29</sup> Therefore,  $k_{cat}$  and  $K'_m$  can be determined from the slope and the vertical intercept of the plot of the equation. The dependences of these parameters on  $V_G$  are evaluated using the  $V_G$ -dependent calibration curves in Figure 3(c) and are shown in Figure 3(d). Figure 3(d) shows that  $k_{cat}$  increases and  $K'_m$  decreases as  $V_G$  is increased.

In general, a bio-catalytic reaction is described as  $E + S \xrightleftharpoons[k_{-1}]{k_1} ES \xrightarrow{k_2} E + P$ , where  $E$  is the enzyme



(or the catalyst), S the substrate, ES the enzyme-substrate complex (bound state) and P the product, the second step is the catalytic step, in which the product is formed and the enzyme returns to its original state. Figure 3(d) shows that increasing  $V_G$  results in a faster conversion process from  $\text{H}_2\text{O}_2$  to water catalyzed by a MP-11 molecule. This is because electron transfer is required to initiate the second step. Therefore, enhanced  $k_{et}$  at the MP-11-electrode interface due to the field results in a higher  $k_{cat}$  ( $= k_2$ ) so that more water molecules are produced and MP-11 molecules return to their unbound state more quickly to be available for the next conversion process. Therefore, the required  $\text{H}_2\text{O}_2$  concentration for the system to reach half of its maximum velocity ( $K'_m$ ) becomes lowered.

In Figure 3(d),  $k_{cat}$  shows a faster increase starting at  $V_G = 0.5$  V, indicating a nonlinear dependence on  $V_G$ . This nonlinearity is likely to be the result of the exponential dependence of  $k_{et}$  on  $\beta$  as shown in Equation (1). The voltage-enhanced reaction kinetics is qualitatively supported by the behavior of  $K'_m$  as shown in Figure 3(d), where  $K'_m$  decreases as  $V_G$  is increased, indicating higher bio-catalytic efficiency. Compared to  $k_{cat}$ ,  $K'_m$  shows a mild nonlinearity. Since  $K'_m$  describes the entire bio-catalytic reaction, i.e.  $K'_m$  depends on  $k_{\pm 1}$  and  $k_2$ , the dissociation of ES to E and S (to MP-11 and  $\text{H}_2\text{O}_2$ ) may be the cause for the mild nonlinearity.

#### IV. CONCLUSIONS

The results reported here show that the reduction of  $\text{H}_2\text{O}_2$  to water catalyzed by MP-11 immobilized on an electrode can be controlled by applying a voltage to the immobilized MP-11. This effect is evidenced by the observations that the reduction currents of the electrode in the presence of  $\text{H}_2\text{O}_2$  increase with  $V_G$  and the  $\text{H}_2\text{O}_2$  calibration curve of the electrode shows a downward shift when  $V_G$  is applied. Furthermore, the kinetic parameters of the conversion process show nonlinear dependences on  $V_G$ , as the result of the controlled interfacial electron transfer brought about using  $V_G$ . The nonlinearity indicates the feasibility of effective controlling the efficiency of a bio-catalytic reaction or a conversion process using a voltage. In view of the presence work on biocatalyzed reduction and previous work on biocatalyzed oxidation,<sup>23</sup> this technique can be used to control a general redox enzymatic reaction with enzymes immobilized on an electrode. Viewing the technique from a different perspective suggests that the experimental setup is in fact a field-effect transistor, whose current-generating mechanism is related to the conversion of an analyte to a product using an enzyme as catalyst with the current being amplified by a voltage applied at a third electrode.

#### ACKNOWLEDGMENTS

This work was supported by American Diabetes Association (Grant number 7-08-RA-191) and Cleveland State University (Research Challenge Award).

- <sup>1</sup> R. A. Marcus, and N. Sutin, *Biochim. Biophys. Acta* **811**, 265 (1985).
- <sup>2</sup> J. Deisenhofer, and J. R. Norris, *The Photosynthetic Reaction Center* (Academic Press Inc., San Diego, 1993), vol. **I**.
- <sup>3</sup> H. B. Gray, and J. R. Winkler, *Proc. Nat. Acad. Sci. U.S.A.* **102**, 3534 (2005).
- <sup>4</sup> D. N. Beratan, J. N. Onuchic, J. R. Winkler, and H. B. Gray, *Science* **258**, 1740 (1992).
- <sup>5</sup> C. C. Page, C. C. Moser, X. Chen, and P. L. Dutton, *Nature* **402**, 47 (1999).
- <sup>6</sup> J. F. Smalley, S. W. Feldberg, C. E. D. Chidsey, M. R. Linford, M. D. Newton, and Y.-P. Liu, *J. Phys. Chem.* **99**, 13141 (1995).
- <sup>7</sup> V. S. Pande, and J. N. Onuchic, *Phys. Rev. Lett.* **78**, 146 (1997).
- <sup>8</sup> J. N. Onuchic, C. Kobayash, O. Miyashita, P. Jennings, and K. K. Baldrige, *Phil. Trans. R. Soc. B* **361**, 1439 (2006).
- <sup>9</sup> J. M. Nocek, J. S. Zhou, S. D. Forest, S. Priyadarshy, D. N. Beratan, J. N. Onuchic, and B. M. Hoffman, *Chem. Rev.* **96**, 2459 (1996).
- <sup>10</sup> M. Alcalde, M. Ferrer, F. J. Plou, and A. Ballesteros, *Trends Biotechnol.* **24**, 281 (2006).
- <sup>11</sup> M. R. Wasielewski, *Chem. Rev.* **92**, 435 (2002).
- <sup>12</sup> G. L. Closs, and J. R. Miller, *Science* **240**, 440 (1988).
- <sup>13</sup> J. R. Winkler, and H. B. Gray, *Chem. Rev.* **92**, 369 (2002).
- <sup>14</sup> M. J. Therien, J. Chang, A. L. Raphael, B. E. Bowler, and H. B. Gray, in *Structure and bonding* (Springer, New York, 1991), pp. 109.
- <sup>15</sup> B. E. Bowler, A. L. Raphael, and H. B. Gray, *Prog. Inorg. Chem.: Bioinorg. Chem.* **38**, 259 (1990).
- <sup>16</sup> B. Durham, L. P. Pan, S. Hahm, J. Long, and F. Millett, in *Electron Transfer in Biology and the Solid State*, edited by M. K. Johnson *et al.* (American Chemical Society, Washington, DC, 1990), pp. 181.

- <sup>17</sup> B. A. Heller, D. Holten, and C. Kirmaier, *Science* **269**, 940 (1995).
- <sup>18</sup> V. L. Davidson, *Biochemistry* **41**, 14633 (2002).
- <sup>19</sup> A. Warshel, and D. W. Schlosser, *Proc. Nat. Acad. Sci. U.S.A.* **78**, 5564 (1981).
- <sup>20</sup> J. L. Willit, and E. F. Bowden, *J. Electroanal. Chem.* **221**, 265 (1987).
- <sup>21</sup> E. Strauss, B. Thomas, and S.-T. Yau, *Langmuir* **20**, 8768 (2004).
- <sup>22</sup> A. Kranich, H. K. Ly, P. Hildebrandt, and D. H. Murgida, *J. Am. Chem. Soc.* **130**, 9844 (2008).
- <sup>23</sup> Y. Choi, and S.-T. Yau, *Anal. Chem.* **81**, 7123 (2009).
- <sup>24</sup> P. Turano, and Y. Lu, in *Handbook on Metalloproteins*, edited by I. Bertini, A. Sigel, and H. Sigel (Marcel Dekker, New York, 2001).
- <sup>25</sup> G. Wang, N. M. Thai, and S.-T. Yau, *Electrochem. Comm.* **8**, 987 (2006).
- <sup>26</sup> J. A. Runquist, and P. A. Loach, *Biochim. Biophys. Acta* **637**, 231 (1981).
- <sup>27</sup> V. Razumas, J. Kazlauskaitė, T. Ruzgas, and J. Kulys, *Bioelectroch. Bioener.* **28**, 159 (1992).
- <sup>28</sup> D. N. Beratan, J. N. Betts, and J. N. Onuchic, *Science* **252**, 1285 (1991).
- <sup>29</sup> See supplementary material at <http://dx.doi.org/10.1063/1.3672093> for the effect of reversing the polarity of VG on the redox properties of immobilized FePP, characterization of MP-11-immobilized electrode, and the Lineweaver-Burk (LB) plot.
- <sup>30</sup> K. Shlgehara, and F. C. Anson, *J. Phys. Chem.* **86**, 2776 (1982).
- <sup>31</sup> E. S. Snow, P. M. Campbell, R. W. Rendell, F. A. Buot, D. Park, C. R. K. Marrian, and R. Magno, *Appl. Phys. Lett.* **72**, 3071 (1998).
- <sup>32</sup> S.-T. Yau, and G. Qian, *Appl. Phys. Lett.* **86**, 103508 (2005).
- <sup>33</sup> S. J. Tans, A. R. M. Verschueren, and C. Dekker, *Nature* **393**, 49 (1998).
- <sup>34</sup> A. J. Bard, and L. R. Faulkner, *Electrochemical Methods* (John Wiley & Sons, New Jersey, 2001), 2 edn.
- <sup>35</sup> M. Wang, F. Zhao, Y. Liu, and S. Dong, *Biosens. Bioelectron.* **21**, 159 (2005).
- <sup>36</sup> F. Mazzei, G. Favero, M. Frasconi, A. Tata, and F. Pepi, *Chem. Eur. J.* **15**, 7359 (2009).
- <sup>37</sup> T. Ruzgas, E. Csoregi, J. Emneus, L. Gorton, and G. Marko-Varga, *Anal. Chim. Acta* **330**, 123 (1996).
- <sup>38</sup> R. A. Kamin, and G. S. Wilson, *Anal. Chem.* **52**, 1198 (1982).
- <sup>39</sup> D. J. Voet, and J. G. Voet, *Biochemistry* (Wiley, New York, 1995), 2 edn.
- <sup>40</sup> A. S. Kumar, and J.-M. Zen, *Electroanalysis* **14**, 671 (2002).